Journal of Computational Science & Engineering 3 (2012) 154-160

Journal of Computational Science & Engineering

Available at http://www.asocse.org ISSN 1710-4068

Electron-Related Oxidation and Reduction on Imidazole Trimer

YangJun, Ding, PeiYing Cui*, BingPing Liu*

School of Chemistry and Chemical Engineering, Qufu Normal University, Qufu, 273165, China

Article Information

Article history:
Received 12 October 2012
Revised 20 October 2012
Accepted 21 October 2012
Available online 25 October 2012

Keywords:
Density functional theory
Geometry optimization
Oxidation and reduction
NBO charges
Ionization potential

Abstract

Density functional theory approach at the B3LYP/6-311++G(d,p) level is employed for the investigation about imidazole trimer system with a special emphasis on the influence upon oxidation and reduction. The influence upon oxidation occurs distinctly on proton donor fragment, and the influence upon reduction is significant for the proton acceptor fragment. It is easier for the neutral trimer to accept one electron than to donate one electron.

1. Introduction

The oxidation and reduction reactions caused by electron detachment and attachment are ubiquitous in chemical and biological systems. The appropriate redox reaction provides the driving force for the chemical process, photosynthesis, and operation of living things. On the other hand, the system is recovered if only the excess electron is detached from the system, which is reduced due to the electron attachment during the previous step. Furthermore, there is no determinate statement on whether the electron is attached or detached at first during the electron transfer process for the conductor.

The coupling of proton chemistry with redox reactions is important in many enzymes and is

* To whom correspondence should be addressed. E-mail: xideliu@163.com pinglysh@gmail.com

2011 © The American Computational Science Society. All rights reserved.

central to energy transfer in biology. The unique ring structure of Imidazole (ImH) permits one proton to be picked up by the bare N atom and the other one to be released from the other N atom. This action has been employed to explain the proton conductivity properties[1-2] of ImH in the solid state and also in the actual biological surrounding where a long H-bonded chain is present, and therefore many investigations have been carried out in both experimental[3-6] and theoretical[7-14] fields in recent years. The ImH-$(HImH)^+$-ImH ($(ImH)_3H^+$) complex has been observed in the experiment[13] about the diffusion mechanism of an excess proton in imidazole molecule chains. The electronic effects on protonated hydrogen-bonded ImH trimer and corresponding derivatives cationized by alkali metals (Li^+, Na^+, and K^+) have also been explored [15].

In our present work, the geometries changes, IR frequency shifts, charge population variations are investigated based on ImH trimer, $(ImH)_3$, with a special emphasis on electronic effects. The following parts are organized in the order of computational details, results and discussions, and the conclusions.

2. Computational Details

The reliability of B3LYP/6-311++G(d, p) level on ImH related systems has been established.[13-15] Thus, the conformation optimizations have been performed based on the hybrid density functioinal theory employing B3LYP function[16-20] with 6-311++G(d, p) basis set. Vibrational frequency analyses are performed at the same level to verify whether the optimized structures correspond to true local minima in the global potential energy surface. The obtained zero-point energy is used in the energy correction for adiabatic electron attachment energy (EA) and the adiabatic ionization potential (AIP). The highest-occupied molecular orbital (HOMO) and the natural bond orbital (NBO) analyses are performed to investigate the charge population on oxidation/reduction by electron detachment/attachment. In present paper all calculations are implemented using the Gaussian 98 program.[21]

3. Results and Discussions

The schemes for $(ImH)_3$ as well as the oxidized and reduced $(ImH)_3$, $(ImH)_3^+$ and $(ImH)_3^-$ are all represented in Fig. 1. The primary optimized geometry parameters are all collected in this figure. The vibrational spectroscopy, one of the standard methods to investigate molecular structures, provides structural information of molecules by detecting molecular vibrations based on the strengths and positions of chemical bonds and interactions. The harmonic vibration IR spectra of these complexes are gathered in Fig. 2. Fig. 3 collects the NBO charge populations for these complexes. The HOMO, the lowest-unoccupied molecular orbital (LUMO), as well as the spin density populations are all shown in Fig. 4.

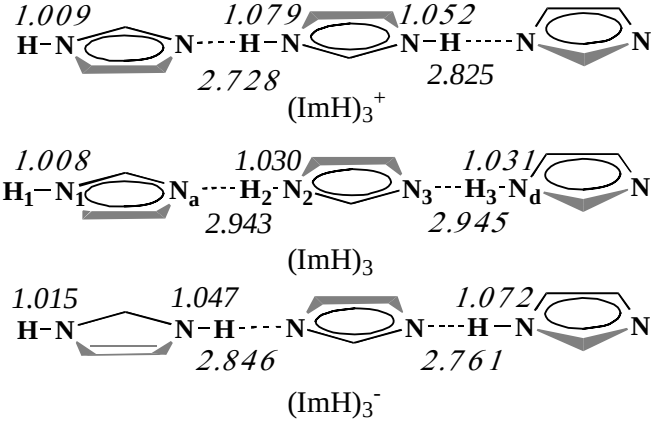

Figure 1 The primary optimized geometry parameters for $(ImH)_3^+$, $(ImH)_3$, and $(ImH)_3^-$. The numberings for cation and anion are same with the neutral.

2011 © The American Computational Science Society. All rights reserved.

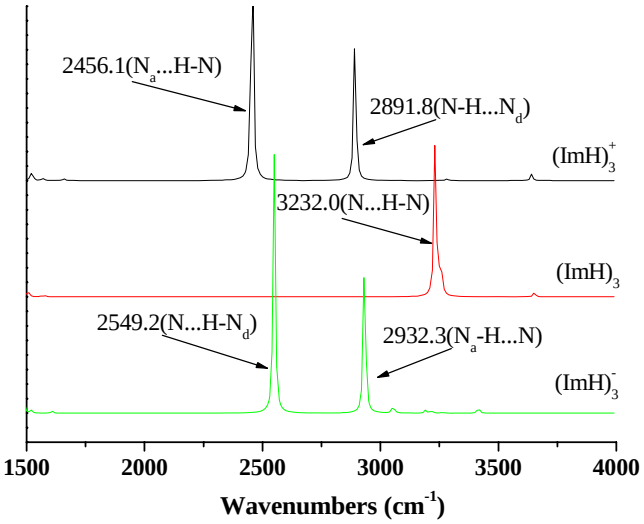

Figure 2 IR Spectra for $(ImH)_3^+$, $(ImH)_3$, and $(ImH)_3^-$ calculated at B3LYP/6-311++G(d, p) Level.

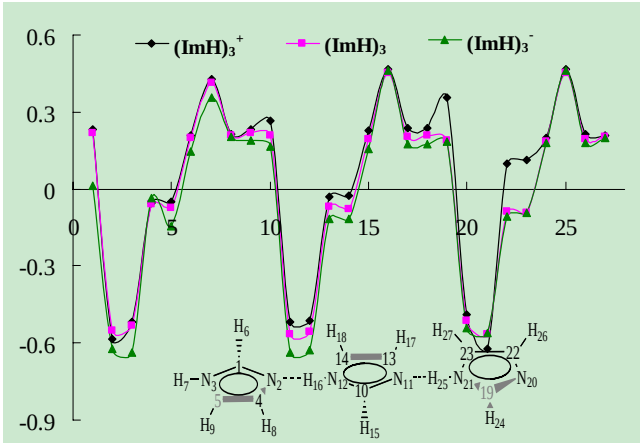

Figure 3 The NBO charge populations on $(ImH)_3^+$, $(ImH)_3$, and $(ImH)_3^-$.

3.1. Geometry Characters

For the neutral ImH trimer, $(ImH)_3$, both the N-H bond of middle ImH fragment (N_2-H_2) and the N-H bond of the right donor ImH fragment (N_d-H_3) are participant of the intermolecular hydrogen bond. Their bonds lengths are elongated as compared with the left N-H bond (N_1-H_1), which is equal to the N-H bond of ImH monomer.[14] These two N-H bonds (N_2-H_2 and N_d-H_3) are almost equal to each other for their similar chemical environment (between two ImH rings). This situation is same for the corresponding intermolecular N…H-N bonds, N_a…H_2-N_2 and N_3…H_3-N_d. The middle ImH fragment is almost perpendicular to the other two terminal ImH fragments, as is in consistent with the phenomenon observed in experiments.[13] Upon oxidation by electron detachment, the proton (H_3) on right donor fragment is transferred completely to the middle ImH, which carries the protonated HImH character because the proton (H_2) on this fragment is only transferred partly. This is verified by the bond length variations of N_3-H_3 (from 1.915Å in $(ImH)_3$ to 1.052Å in $(ImH)_3^+$) and N_2-H_2 (from 1.030Å in $(ImH)_3$ to 1.079Å in $(ImH)_3^+$). While the changes of left N-H bond on the acceptor ImH fragment upon oxidation is very weak. The other distinct changes caused by electron detachment is the shortening of two intermolecular N-H…N distances, especially for the N_a…H_2-N_2 bond. Therefore, the influence to the donor fragment is more significant than the influence to the acceptor fragment upon oxidation. When the excess electron is attached on the system, the proton (H_2) on middle ImH fragment is transferred to left acceptor ImH fragment, instead of the proton (H_3) on right donor ImH fragment, which is only lengthened from 1.031Å to 1.072Å. The original planar structure determined by left acceptor ImH molecular framework is broken because the H_1 departs from the plane. The N_1-H_1 bond length increases from 1.008Å to 1.015Å. The intermolecular N-H…N hydrogen bonds decrease from 2.943Å to 2.846Å for N_a…H_2-N_2 and from 2.945Å to 2.761Å for N_3…H_3-N_d. Totally, the variations on reduction generated by electron attachment are more significant for the acceptor fragment, instead of the donor part. As is opposite as compared with the influence caused by oxidation. Although the molecule reorganizes upon oxidation and reduction, the length of the whole framework

2011 © The American Computational Science Society. All rights reserved.

(the N_1…N distance) only slightly changes between 11.8Å and 11.6Å.

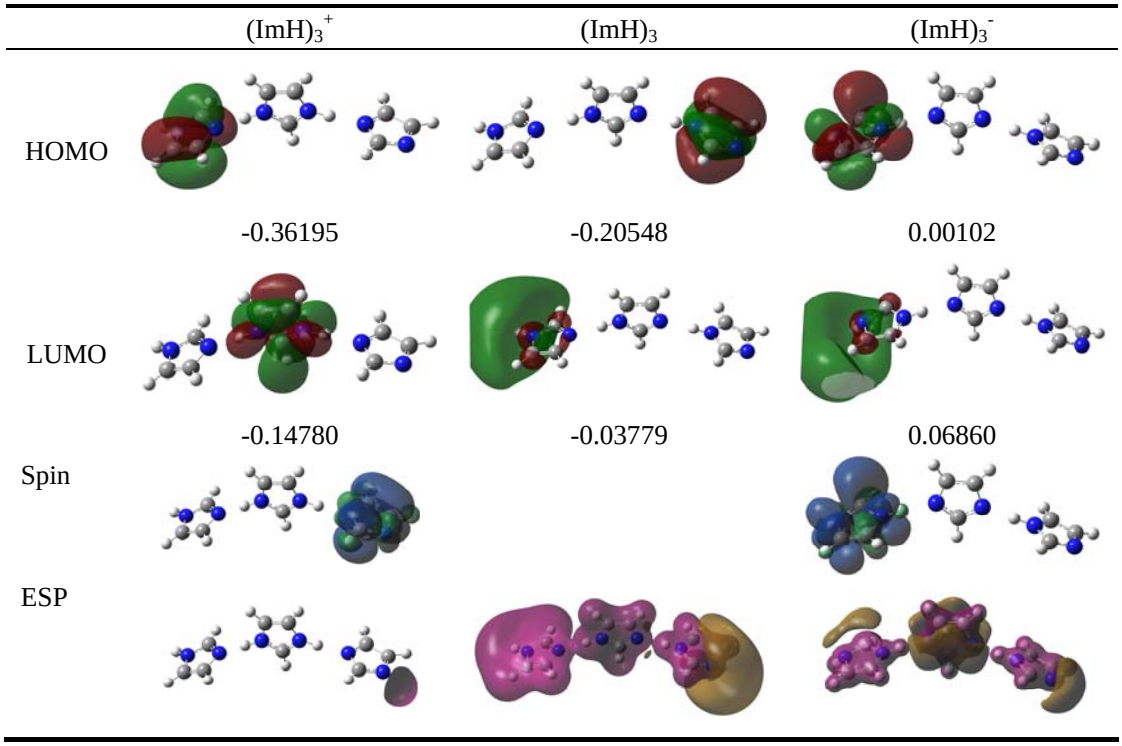

Figure 4 The HOMO, LUMO, spin, and ESP of $(ImH)_3^+$, $(ImH)_3$, and $(ImH)_3^-$.

3.2. IR Frequencies

The infrared vibrational frequency analyses are performed to get some structural information as well as to validate whether they corresponding to the local minima or not. The primary vibrational frequencies of $(ImH)_3$ are represented in Fig. 2. For comparison, the IR frequencies of the corresponding oxidized as well as the reduced complexes are all collected in this figure. It can be observed from Fig. 2 that the vibrational frequencies of two intermolecular N-H…N H-bonds (N_a…H-N and N…H-N_d) are superposed together (3232.0 cm^{-1}). This also demonstrates their similar chemical environments. As compared with the intermolecular N-H…N H-bonds in ImH dimer ($(ImH)_2$) investigated in ref 14, the intermolecular of $(ImH)_3$ is red-shifted by about 130 cm^{-1}. Upon oxidation, the IR frequencies of two N-H…N H-bonds are red-shifted significantly, especially for the H-bond between left acceptor fragment and the middle bridging ImH, which is red-shifted by 776 cm^{-1}. The frequencies of the intermolecular H-bond between right donor part and the middle bridging ImH fragment is blue-shifted as compared with the oxidized $(ImH)_2$, $(ImH)_2^+$, by ~ 170 cm^{-1}.[14] The red-shift also can be observed for these two intermolecular H-bonds upon reduction. While for the reduced triad, $(ImH)_3^-$, the N-H…N H-bond between the right donor ImH ring and the middle ImH fragment red-shifts more significantly as compared with the N-H…N bond between the acceptor and the middle ImH fragments. Through the above analyses, we also

2011 © The American Computational Science Society. All rights reserved.

can get the conclusion that the influence upon oxidation and reduction to the system is opposite. In other words, significant influence is brought upon oxidation to right donor ImH fragment, while upon reduction by electron attachment, prominent variations is found at the left acceptor ImH ring.

3.3. NBO Populations

NBO charge populations on $(ImH)_3^+$, $(ImH)_3$, and $(ImH)_3^-$ are all represented in Fig. 3 for the convenience of comparison. From this figure, it can be easily observed that all the nitrogen atoms of the neutral $(ImH)_3$ carry significant negative charges (~ -0.55 e). The C=C groups also share a little negative charges (~ -0.05 e). The positive charges locate predominantly on the H atoms which are bonded with N (~ 0.45 e). The other H atoms and the bridging carbon atoms of two N atoms in every ImH ring possess about 0.25 e. It also can be seen that the NBO charges populate on three ImH fragments almost averagely and periodically (every 9 atoms). The charge population on left acceptor ImH fragment only changes weakly upon oxidation. The NBO charges located on the H atoms of middle bridging ImH ring vary slightly upon electron detachment. Similarly, no significant alteration is observed for the NBO charge population of the right donor fragment. While the positive charge increases and the negative value decreases for the framework N and C atoms of bridging ImH as compared with the data of neutral trimer. The positive charges localized on the bridging C of two N atoms of the donor fragment is enhanced distinctly (~ 0.16 e). The negative charges populated on N_d increases by 0.06 e. Another intriguing phenomenon can be observed is the charge population on C=C group, which changes from negative (-0.1 e) to positive (0.1 e). Here, it is obvious that the variation occurred upon oxidation on right donor ImH fragment is more significant as compared with that on left acceptor fragment.

While upon reduction, the situation is quite different. Similar to the phenomenon upon oxidation, the NBO charges populated on the H atoms bonded with two N atoms of the bridging ImH ring also vary very weakly upon reduction by electron attachment. While the NBO charge alterations upon reduction of the framework C and N atoms of the bridging ImH ring are opposite as compared with the variations upon oxidation, the positive charge is decreasing and the negative charge is increasing. As compared with the changes upon oxidation, the other significant difference can be observed upon reduction is the variation of three ImH rings. In other words, the variations of the donor ring are slight and the changes of the acceptor ImH fragment are distinct. Especially, the NBO charges located on the bridging C atom of two N atoms of left acceptor fragment decreases near to zero.

The analyses about the highest-occupied molecular orbital (HOMO) and the lowest-unoccupied molecular orbital (LUMO) also present some useful information. As shown in Fig. 4, two electron occupied HOMO orbital of $(ImH)_3$ locates on the right donor ImH fragment and the unoccupied LUMO orbital populates on the left acceptor ImH fragment. Therefore, the electron detachment (oxidation) should be occurred on the right donor fragment and the electron should be attached on the left acceptor ImH ring upon reduction. This conclusion also is supported by the spin population represented in Fig. 4. After electron detachment, the odd electron is left on the right ImH fragment. The unpaired electron is located on the right ImH ring upon electron attachment. After oxidation or reduction, the property of the

2011 © The American Computational Science Society. All rights reserved.

system also varies significantly, as can be seen from the electrostatic potential (ESP) collected in Fig. 4.

With the above analyses, we can conclude safely that the influence to different fragments upon oxidation or reduction by electron detachment or attachment is distinct. Therefore, it is significant to clarify the first step is electron attachment or electron detachment on earth in the electron transport process for ImH chain. To resolve this problem, we perform the calculations about the adiabatic electron attachment energy (E_A) and the adiabatic ionization potential (AIP) of $(ImH)_3$.

3.4. E_A and AIP

On the same level, we calculated the E_A and the AIP of $(ImH)_3$ in order to inspect which one is more difficult to occur for the oxidation and the reduction. After zero-point vibrational energy correction, the E_A of $(ImH)_3$ is only 1.2 kcal/mol, while the AIP is 159.0kcal/mol. It should be easier for the neutral ImH trimer to accept the electron in the first step than to donate one electron. Therefore, in the electron transport process for the ImH chain, the first step is to accept one electron by the proton donor ImH fragment. Then, the electron is transferred in the chain along with the proton move to the proton acceptor ImH ring.

4. Conclusion

The geometry changes, frequency shifts, NBO charge variations, as well as the energy alterations upon oxidation and reduction are explored with the density functional theory approach at B3LYP/6-311++G(d,p) level. The influence to the proton donor ImH fragment upon oxidation is significant, while the influence to the proton acceptor ImH ring upon electron attachment is distinct. The first step in the electron transport process for the ImH chain should be the acceptance of excess electron.

References

[1] J. T. Daycock, G. P. Jones, J. R. N. Evans, J. M. Thomas, Nature, 218, (1968) 672.
[2] A. Kawada, A. R. McGhie, M. M. Labes, J. Chem. Phys. 52, (1970) 3121.
[3] L. Colombo, P. Bleckmann, B. Schrader, R. Schneider, Th. Plesser, J. Chem. Phys. 61, (1974) 3270.
[4] P. W. Loeffen, R. F. Pettifer, F. Fillaux, G. J. Kearley, J. Chem. Phys. 103, (1995) 8444.
[5] B. S. Hickman, M. J. J. Mascal, Titman, I. G. Wood, J. Am. Chem. Soc. 121, (1999) 11486.
[6] C. C. Su, H. C. Chang, J. C. Jiang, P. Y. Wei, L. C. Lu, S. H. Lin, J. Chem. Phys. 119, (2003) 10753.
[7] H. Chojnacki, J. Lipinski, Adv. Mol. Relax. Interaction Processes, 18, (1980) 149.
[8] H. Basch, M. Krauss, W. J. Stevens, J. Am. Chem. Soc. 107, (1985) 7267.
[9] F. B. C. Machado, E. R. Davidson, J. Chem. Phys. 97, (1992) 1881.
[10] P. I. Nagy, G. J. Durant, D. A. Smith, J. Am. Chem. Soc. 115, (1993) 2912.
[11] S. Scheiner, M. Y. Yi, J. Phys. Chem. 100, (1996) 9235.
[12] W. Tatara, M. J. Wójcik, J. Lindgren, M. Probst, J. Phys. Chem. A. 107, (2003) 7827.
[13] W. Münch, K. D. Kreuer, W. Silvestri, J. Maier, G. Seifert, Solid State Ionics. 145, (2001) 437.
[14] S. Yan, Y. Bu, J. Phys. Chem. B. 108, (2004) 13874.
[15] S. Yan, Y. Bu, P. Li, J. Chem. Phys. 122, (2005) 054311.

2011 © The American Computational Science Society. All rights reserved.

[16] A.D. Becke, J. Chem. Phys. 98 (1993) 5648.

[17] C. Lee, W. Yang, R.G. Parr, Phys. Rev. B 37 (1988) 785.

[18] Sun, W. J. Comput. Sci. Eng. 2011, 1, 54.

[19] P. Cui, B. Liu, J. Comput. Sci. Eng. 2011, 104.

[20] H. Ma, S. Yan, L. Bai, S. Bi, J. Comput. Sci. Eng. 2012, to be published.

[21] Frisch, M. J.; Trucks, G. W.; Schlegel, H. B.; Scuseria, G. E.; Robb, M. A.; Cheeseman, J. R.; Zakrzewski, V. G.; Montgomery, J. A.; Stratmann, Jr., R. E.; Burant, J. C.; Dapprich, S.; Millam, J. M.; Daniels, A. D.; Kudin, K. N.; Strain, M. C.; Farkas, O.; Tomasi, J.; Barone, V.; Cossi, M.; Cammi, R.; Mennucci, B.; Pomelli, C.; Adamo, C.; Clifford, S.; Ochterski, J.; Petersson, G. A.; Ayala, P. Y.; Cui, Q.; Morokuma, K.; Malick, D. K.; Rabuck, A. D.; Raghavachari, K.; Foresman, J. B.; Cioslowski, J.; Ortiz, J. V.; Stefanov, B. B.; Liu, G.; Liashenko, A.; Piskorz, P.; Komaromi, I.; Gomperts, R.; Martin, R. L.; Fox, D. J.; Keith, T.; Al-Laham, M. A.; Peng, C. Y.; Nanayakkara, A.; Gonzalez, C.; Challacombe, M.; Gill, P. M. W.; Johnson, B.; Chen, W.; Wong, M. W.; Andres, J. L.; Gonzalez, C.; Head-Gordon, M.; Replogle, E. S.; Pople, J. A. Gaussian, Inc., Pittsburgh PA, 1998.

2011 © The American Computational Science Society. All rights reserved.